

## Comparison of Virtual Globe technologies for depiction of radar beam propagation effects and impacts

Scott T. Shipley\*

George Mason University, Fairfax, Virginia

Randy M. Steadham and Daniel S. Berkowitz

NOAA/NEXRAD Radar Operations Center, Norman, Oklahoma

### 1. INTRODUCTION

Virtual Globes (VGs) are quickly becoming the new paradigm in the Earth Sciences for education and outreach, logistics, and data access. VGs such as Google Earth, NASA WorldWind, ESRI ArcGIS Explorer, Microsoft Virtual Earth and many others are changing how science professionals and the public view and access geographic information, including observations and forecasts for applications in meteorology and climate, oceanography, and hydrology. We demonstrate the capabilities of VG platforms for representation of radar beam elevation above the Earth surface. Effects and impacts addressed include beam occultation by terrain, anomalous propagation, and the potential interaction of radar systems with wind power generators.

Several methods for the display of radar-derived information in three dimensions were prototyped and tested, the goal being to depict and visualize true geographic position. VG technology can be used to convey information about radar beam properties and effects in a geographically familiar manner with an easy-to-use human interface. VG systems are fast and efficient, and combine 3D perspective with rapid user-defined motion to explore regions of interest. The use of semi-transparent image layers allow an observer to integrate spatial information from disparate sources, and to intuitively discover the impact of complex physical processes and variations in the vertical dimension. The user experience is pleasant and even fun, and users find it easy to relate complex information to personal knowledge in their own areas of interest.

VG technologies are well adapted to convey radar beam occultation by obstacles to propagation (e.g.

\* Corresponding author address:

Scott T. Shipley, Dept of Geography, MS 1E2  
4400 University Drive, Fairfax, VA 22030-4444  
e-mail: [sshipley@gmu.edu](mailto:sshipley@gmu.edu)

*The views expressed are those of the authors and do not necessarily represent those of NOAA nor George Mason University.*

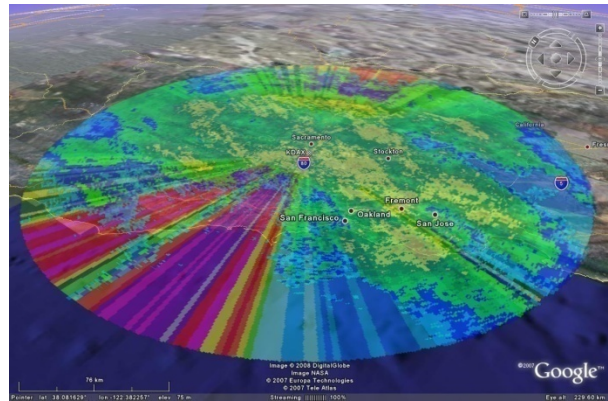


**Figure 1** – 3D Occultation pattern at  $0.5^\circ$  elevation for NEXRAD at Sacramento, CA (KDAX), overlaid with radar reflectivity at 1825 UTC on 4 January 2008.

terrain), and the altitude of the radar beam above the ground. Conventional 2D depictions drape radar and other data on the surface as a “ground overlay”. Of the various methods tested for this study (e.g. 3D point plotting, vertical cross sections, etc.), the best overall performance was achieved by draping 2D images on elevated surfaces or “models” assuming standard radar beam propagation, and adjusting these model surfaces to the correct height using known radar parameters. The model is an arbitrary vertical terrain constructed using a Triangulated Irregular Network (TIN), and was developed for this study using the approach detailed by Shipley et al. (2005).

Complete details of the function and operation of the NEXRAD radar system can be found in the Federal Meteorological Handbook No. 11 (2005 and updates). Methods to estimate radar beam occultation have been described by Maddox et al. (2002), Shipley et al. (2005, 2006), and others. The original method for siting the NEXRAD system is documented by Leone et al. (1989). The occultation method employed for this paper uses ESRI ArcGIS to calculate radar beam height above the Earth surface on a cell by cell basis. The radar spatial calculation is performed at 1 km radial range by 1 degree azimuth, sampled over

the National Geophysical Data Center 30 arcsec digital terrain database, cf. Graffman (2004).

At the time of this publication, our most advanced VG results are available as \*.kmz files for Google Earth. Sample kmz files are available on-line at <http://wxanalyst.com/radar/>. These sample kmz files are freely available for public use. Caution should be exercised, however, in the interpretation and use of these results. *The occultation method employed is a 2<sup>nd</sup> order approximation, and should be used only to convey the general characteristics of radar beam occultation. Results are not exact. Spatial quality of the results is limited to quality of the databases available and the assumptions made.*

## 2. NAVIGATING THE TEST kmz

A sample 3D structure for radar reflectivity and occultation is shown in Figure 1 for Sacramento, CA (KDAX) using a single kmz file (200 kByte) for Google Earth. Similar depictions have been tested or are under development for other VGs including the ESRI ArcGIS Explorer, NASA Worldwind, and Microsoft Virtual Earth. The Google Earth method is described here to illustrate the overall capability of Virtual Globe technologies for radar applications.

The Google Earth 4.2 (beta) VG is freely available at <http://earth.google.com/> for PC, Mac and Linux. Once this application is installed, data files with the extension \*.kml (text) or \*.kmz (compressed) should load to or start Google Earth automatically. The sample kmz used in this paper are available at <http://wxanalyst.com/radar/>, as follows:

wx_radars.kmz	Information on 155 U.S. NEXRAD systems.
Knnnvv.kmz	Individual radar models and sample data, with links to NWS Ridge; nnn is the 3-letter radar designation, and vv is file version.
mosaicx.kmz	Regional mosaics of radar "floor", or lowest sampled elevation for a network of weather radars.

Figure 2 enumerates the layer structure of the kmz file for KDAX (Sacramento, CA), which is shown in Figure 1. Individual layers in this kmz are associated with geographic structures identified in Figure 2 by the following symbols:

	kmz document		radar tower point
	model layer		ground overlay

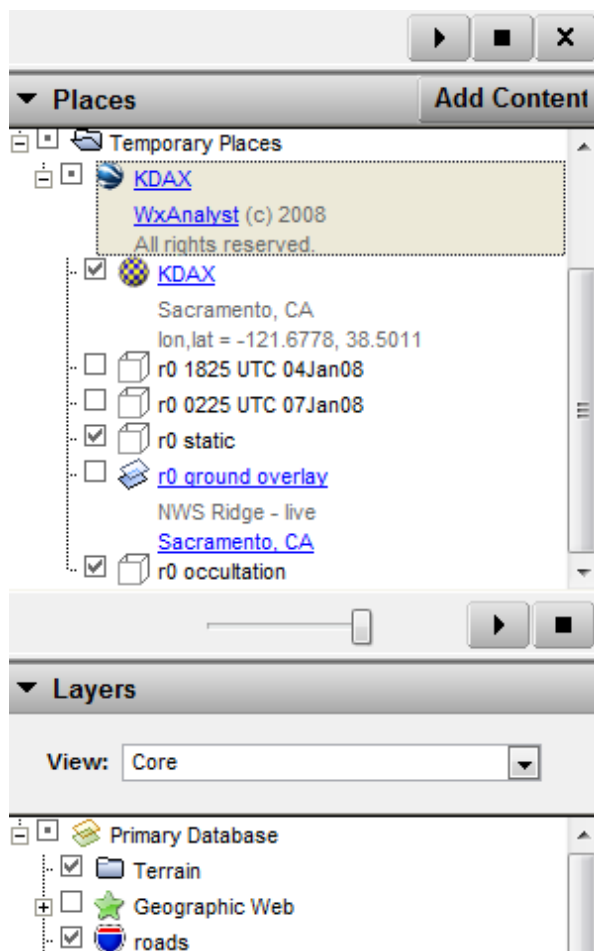


**Figure 2** – Structure of the file kdax9e.kmz displayed in Figure 1, as shown in the legend of Google Earth. This structure depicts the lowest level scan surface (0.5 degrees elevation) of the Sacramento, CA (KDAX) weather radar.

The highlighted text (e.g. [KDAX](#)) is a hyperlink, which may provide additional information or link the user to an external web page.  [KDAX](#) moves the VG to a position just above the radar at close range, as shown in Figure 3. This feature locates the radar, which is often visible in the VG imagery. The shadow of the KDAX radar structure is visible in GE imagery, as shown in the inset of Figure 3. The  models are images draped on a COLLADA model representing the 3D surface of the 0.5° elevation scan. Sample images are provided for specific precipitation events, as well as a live link to NWS Ridge (r0 static). Due to the limitations of KML 2.2, the r0 static layer does not update at this time, but animation should be supported when and if KML is enhanced to include “dynamic skinning”. Finally, a ground overlay  is provided for the NWS Ridge product for comparison. The ground overlay updates every 5 minutes.



**Figure 3** – Cone of silence over KDAX. The inset shows a close-up of the KDAX radar tower. Double click the KDAX point layer symbol  to zoom into the radar tower area.

3D structure can be seen in Google Earth provided that the terrain checkbox is checked in the Primary Database, see Layers section of Legend at the bottom of Figure 2. The 3D perspective images in this paper were created with terrain enabled and vertical exaggeration set to 1.

Layer r0 occultation  for KDAX is shown in Figure 4 for the lowest beam elevation angle, which is nominally about one half degree. The radar is also elevated approximately 10 m above the surface. Beam altitude above the Earth geoid is affected by beam elevation angle, curvature of the Earth, and anomalous propagation (see Shipley et al., 2007). Figure 4 shows theoretical reduction in beam cross section as beam area is truncated by terrain. Simply put, the Earth surface (also vegetation and manmade obstacles) removes energy from the radar beam upon intersection, and a “shadow” of the obstacle propagates with the beam to longer ranges. The color scheme defined in Figure 5 is employed to indicate percentage of available beam area, which we call “occultation”. The color scheme has been selected for fast and intuitive interpretation. Occultation patterns associated with blues and greens indicate beam cross section reductions of less than half. The reds indicate substantial beam cross section reductions of more than half. Since this image is draped on a model surface which represents the vertical beam centroid, reds should also be associated with terrain features that intersect this surface, as shown in Figures 6.

### 3. ANALYSIS OF BEAM OCCULTATION

Intersection of the KDAX r0 occultation layer with the Sierra Nevada range is shown in Figures 6a and 6b. Orange (40%) and red (30%) layer colors

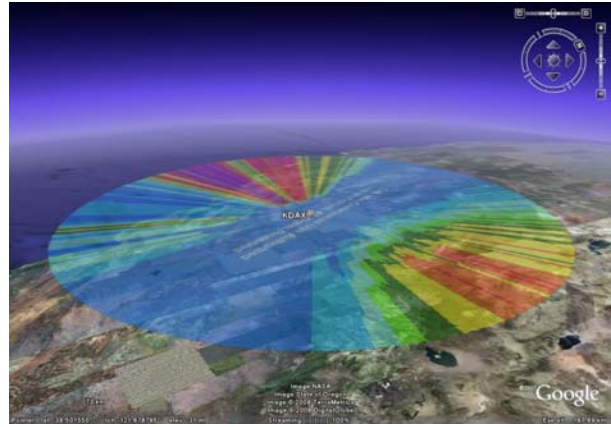


**Figure 4** – Occultation pattern for Sacramento, CA (KDAX). Double click the r0 occultation layer  to move to this perspective.

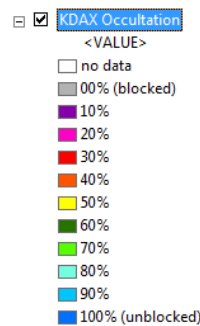


**Figure 5** – Occultation key for percentage available area of the radar beam cross section. Terrain and other obstacles can reduce available beam area over the radar beam propagation path.

are associated with beam truncation above the beam centroid, which is consistent with terrain “poking through” all r0 layers in the sample kmz files. To see data which may be obscured by terrain, simply uncheck the terrain checkbox.

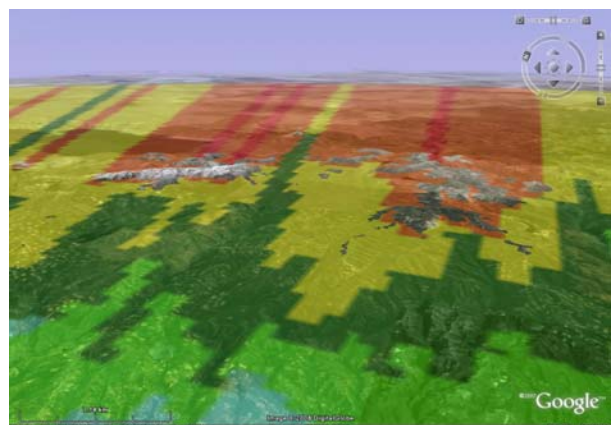


**Figure 6a** – Occultation of KDAX by the Sierra Nevada. Compare to figure 6b on next page.

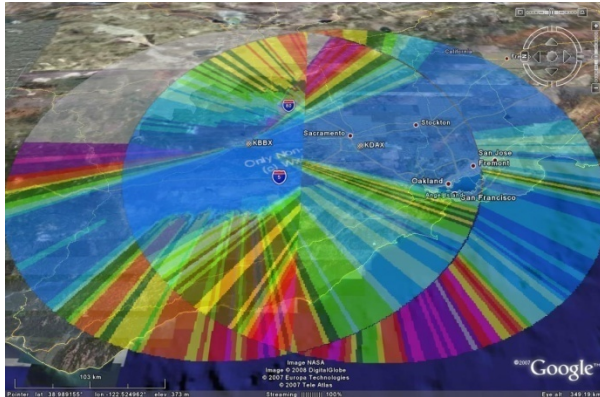


**Figure 7** – Juxtaposition of r0 occultation patterns for two adjacent radars (KDAX from Figure 4, and Beale AFB in Oroville, CA (KBBX). Note that KBBX is 100% blocked in its northeast sector.

The impact of beam truncation to signal strength can be easily seen in Figure 6b, and better understood by animating Figures 6a and 6b (i.e., switch pages in this document to alternate 6a and 6b, or load kdax9e.kmz and click layer visibility for “r0 1825 UTC 4jan2008” on and off). Notice how precipitation echo strength is greater through and behind gaps in terrain, and is relatively weaker in the “shadow” of terrain features. It is obvious from these images that terrain features are reducing beam cross section, and therefore reducing the signal strength of precipitation which may otherwise be filling the theoretical beam area. Since terrain removes cross section from the bottom of the radar beam, it also follows that low-level precipitation may go undetected behind such shadows or at the larger ranges where the beam is elevated significantly above the Earth surface.

VG technology is fast enough to support visualization and analysis of multiple adjacent radars. As shown in Figure 7, the juxtaposition of two adjacent radars enables geographic investigation of radar data voids, or regions where no radar coverage is provided by the current network. Such voids can be reduced by re-siting existing radars or by enhancing the existing network with additional radar systems. In addition, this technique supports additional vertical layers, such as the higher altitude scans provided by the r1, r2 and r3 elevations.

It is important to note that these occultation patterns have been calculated assuming normal (standard) beam propagation. The radar beam is refracted by the atmosphere, where radio refractive index is primarily dependent on the vertical structure of humidity and temperature. Other atmospheric conditions can lead to anomalous propagation, such as super-refraction,

where the beam path is lower in altitude and may provide anomalous “signals” due to scattering by the Earth surface. Sub-refraction is associated with drier than normal conditions, and results in beam paths that are higher than normal. Anomalous Propagation is well understood, but there is little capability currently provided for AP measurement in the operational system.

#### 4. ANALYSIS OF WIND POWER IMPACT

Wind power generators are known to generate spurious signals or interference in weather radar depictions, showing up in both the reflectivity and velocity products. VG technologies provide a convenient platform for communication with the wind power community, since VG use is widespread in the general population, and the behavior of radar systems can be depicted and explained in a non-technical and easily comprehended manner. Contrast, for example, the 3D radar mosaic in Figure 8, showing the lowest detected altitude of all five radars bracketing the Front Range in Colorado and Wyoming, with the same information shown as a ground overlay in Figure 9a. Figure 8 is better at conveying the vertical structure of the radar detection field, but lacks geographic keys that allow users to pinpoint where a wind power generator may intersect the radar beam field of detection. Non-technical individuals can easily use a VG display, such as that shown in Figures 9a and 9b, to see if their location poses a threat to weather radar operations. Known locations of wind power generators are indicated by placemarks (the pushpins) in Figures 9a and 9b, where color of the ground overlay is used to convey altitude of the radar beam network above the Earth surface.

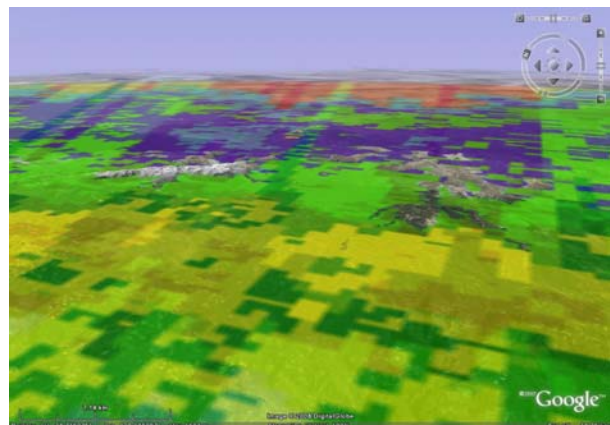


**Figure 6b** – Same as Fig 6a but with data from 4 Jan 08. Flip or switch pages see correlation.

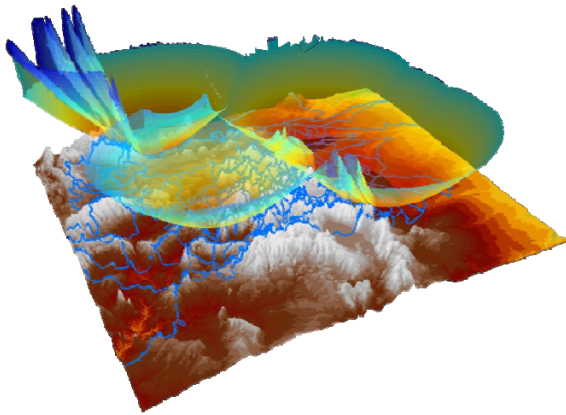


**Figure 8** – Lowest detectable altitude or “floor” for weather radar coverage over the Front Range of CO and WY, from Shipley et al. (2006). A ground overlay of this coverage is shown in Figure 9a. This view was generated by ArcScene under ESRI ArcGIS 9.2.

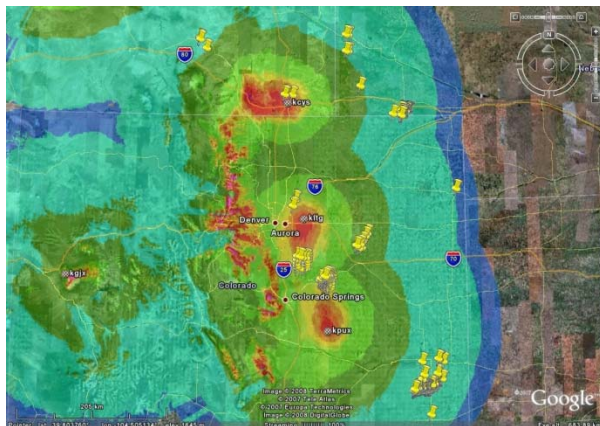


**Figure 9a** – Lowest detectable altitude or “floor” for weather radar coverage over the Front Range of CO and WY. Reds indicate regions where the beam floor is close to the surface. Placemarks indicate the locations of known wind power generators.

Again, reds (beam centroid within 200m of surface) are used to convey areas of significant threat. The mosaic in Figure 9a uses the combined occultation patterns (e.g. Figure 4) for all levels to remove those regions where the radar signal has been blocked by terrain. A closer look to a sensitive area is provided in Figure 9b, which zooms into the placemarks just north of Cheyenne, WY (KCYS). Two of the five indicated wind turbines are visible, which points out the age of the imagery which may be available to a VG.

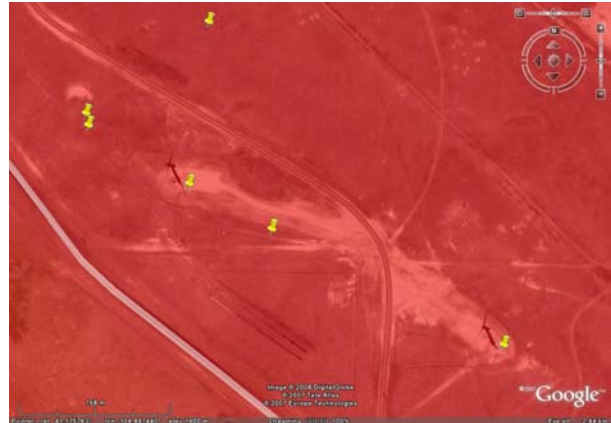


**Figure 9b** – Close up of wind power generators in Google Earth imagery north of Cheyenne, WY (KCYS).

## 5. CONCLUSIONS

Our prototyping and development address the display and analysis of weather radar using Virtual Globe technologies, specifically for ESRI ArcGIS and ArcGIS Explorer, Google Earth, NASA Worldwind, and Microsoft Virtual Earth. 3D depictions of weather radar features are supported by all VG platforms addressed. In addition, these VG technologies are evolving so rapidly, that additional features are expected in the very near future.

## 6. ACKNOWLEDGMENTS

Google Earth version 4.2.0198.2451 (beta) and ESRI ArcGIS 9.2 were used to create the images in this paper. We wish to thank Ira Graffman (NOAA/NWS), Steve Ansari (NOAA/NCDC), and Ron Guenther (RSIS) for their intellectual contributions. Dr. Shipley also thanks WxAnalyst for its generous support.

## 7. REFERENCES

- Federal Meteorological Handbook No. 11, Part B, Doppler Radar Theory and Meteorology (2005), FCM-H11B-2005, as updated, <http://www.ofcm.gov/fmh11/fmh11B.htm>
- Complete information can be found at the Office of the Federal Coordinator for Meteorology (OFCM), <http://www.ofcm.gov/homepage/text/pubs.htm>
- Graffman, I.A., 2004: AWIPS Map Database Home, <http://www.nws.noaa.gov/geodata/>
- Leone, D.A., R.M. Endlich, J. Petročeks, R.T.H. Collis and J.R. Porter, 1989: Meteorological Considerations Used in Planning the NEXRAD Network. *Bull. Amer. Meteor. Soc.*, **70**, 4-13. [http://ams.allenpress.com/pdfserv/10.1175/1520-0477\(1989\)070<0004:MCUIPT>2.0.CO;2](http://ams.allenpress.com/pdfserv/10.1175/1520-0477(1989)070<0004:MCUIPT>2.0.CO;2)

Maddox, R.A., J. Zhang, J.J. Gourley, and K.W. Howard, 2002: Weather radar coverage over the contiguous United States. *Wea. Forecasting*, 17, 927-934.

Shiple, S.T., Graffman, I.A., and R.E. Saffle, 2005: Weather Radar Terrain Occultation Modeling using GIS, Paper J9.5, 21<sup>st</sup> IIPS, AMS Annual Meeting, San Diego, CA.  
[http://ams.confex.com/ams/Annual2005/techprogram/paper\\_87245.htm](http://ams.confex.com/ams/Annual2005/techprogram/paper_87245.htm)

Shiple, S.T., Graffman, I.A., and R.E. Saffle, 2006: GIS Tools for Radar Siting and Analysis. Paper J11.3, 22<sup>nd</sup> IIPS, AMS Annual Meeting, Atlanta, GA.  
[http://ams.confex.com/ams/Annual2006/techprogram/paper\\_104269.htm](http://ams.confex.com/ams/Annual2006/techprogram/paper_104269.htm)

Shiple, S.T., R.E. Saffle and M.H. Jain, 2007: Investigation of point echoes from GPS-enabled aircraft to detect anomalous propagation, Paper 5B.8, 23<sup>rd</sup> IIPS, San Antonio, TX.  
[http://ams.confex.com/ams/87ANNUAL/techprogram/paper\\_120105.htm](http://ams.confex.com/ams/87ANNUAL/techprogram/paper_120105.htm)